Regular Article

Mohamed Abdelsabour Fahmy* and Mohammed M. Almehmadi

Boundary element analysis of rotating functionally graded anisotropic fiber-reinforced magneto-thermoelastic composites

https://doi.org/10.1515/eng-2022-0036
received February 13, 2022; accepted March 23, 2022

Abstract: The primary goal of this article is to implement a dual reciprocity boundary element method (DRBEM) to analyze problems of rotating functionally graded anisotropic fiber-reinforced magneto-thermoelastic composites. To solve the governing equations in the half-space deformation model, an implicit–implicit scheme was utilized in conjunction with the DRBEM because of its advantages, such as dealing with more complex shapes of fiber-reinforced composites and not requiring the discretization of the internal domain. So, DRBEM has low RAM and CPU usage. As a result, it is adaptable and effective for dealing with complex fiber-reinforced composite problems. For various generalized magneto-thermoelasticity theories, transient temperature, displacements, and thermal stresses have been computed numerically. The numerical results are represented graphically to demonstrate the effects of functionally graded parameters and rotation on magnetic thermal stresses in the fiber direction. To validate the proposed method, the obtained results were compared to those obtained using the normal mode method, the finite difference method, and the finite element method. The outcomes of these three methods are extremely consistent.

Keywords: boundary element method, rotation, functionally graded materials, anisotropic, fiber reinforced, magneto-thermoelasticity

*** Corresponding author: Mohamed Abdelsabour Fahmy,** Department of Mathematics, Jamoum University College, Umm Al-Qura University, Alshohdaa 25371, Jamoum, Makkah, Saudi Arabia; Faculty of Computers and Informatics, Suez Canal University, New Campus, 41522 Ismailia, Egypt, e-mail: maselim@uqu.edu.sa
Mohammed M. Almehmadi: Department of Mathematical Sciences, Faculty of Applied Sciences Umm Al-Qura University, Makkah 24381, Saudi Arabia

Nomenclature

β_{ab}	stress–temperature coefficients
δ_{ij}	Kronecker delta $(i,\ j = 1,\ 2)$
μ	magnetic permeability
ρ	density
σ_{ab}	mechanical stress tensor
τ_{ab}	Maxwell's stress tensor
τ	time
$\tau_0,\ \tau_1,\ \tau_2$	relaxation times
ω	uniform angular velocity
$\Psi_f,\ \delta_f,\ f,\ \bar{h}$	prescribed functions
Å	unified parameter
B_i	magnetic strength components
c	specific heat capacities
C_{abfg}	constant elastic moduli
H_i	magnetic field intensity
H_0	constant magnetic field
h	perturbed magnetic field
k_{ab}	thermal conductivity coefficients
k_0	Seebeck coefficient
m	functionally graded parameter
T	temperature
T_0	reference temperature
$\bar{t}_a$	$=\sigma_{ab} n_b$ tractions
u_k	displacement vector

1 Introduction

Biot [1] has developed the classical coupled theory of thermoelasticity to overcome the first shortcoming in the classical theory of thermoelasticity proposed by Duhamel [2] and Neuman and Meyer [3] where it predicts two phenomena that are not consistent with physical observations. First, the heat conduction equation of this theory does not consider any elastic deformation. Second, the heat conduction equation of this theory is of a parabolic form, predicting the infinite velocity of heatwaves' propagation.

Most of the approaches that have emerged to resolve the unacceptable prediction of the classical theory are based on the general notion of heat flux relaxation in the classical Fourier heat conduction equation, thus generating a non-Fourier effect. One of the simplest forms of this equation is due to the extended thermoelasticity theory of Lord and Shulman [4], which is also known as the theory of generalized thermoelasticity with one relaxation time. Another form of this equation is the developed temperature-rate-dependent thermoelasticity theory of Green and Lindsay [5], which is often referred to as the theory of generalized thermoelasticity with two relaxation times. After that, Green and Naghdi [6,7] developed three models for generalized thermoelasticity: model I corresponds to classical heat conduction theory based on Fourier's law, model II corresponds to the thermoelasticity without energy dissipation, and model III corresponds to the thermoelasticity with energy dissipation.

In recent years, thermoelastic problems of functionally graded anisotropic (FGA) composites have gained popularity. In general, finding an analytical solution to a problem is extremely difficult; therefore, several engineering papers devoted to numerical methods have studied such problems in various thermoelasticity topics, for example, coupled thermoelasticity [8], magneto-thermoelasticity [9], couple stress theory [10], nanostructures [11], micropolar piezothermoelasticity [12], micropolar magneto-thermoviscoelastic [13], magneto-thermoviscoelastic [14], transient thermal stresses [15,16], transient thermoelasticity [17], heat conduction [18], and magneto-electroelasticity [19]. But generally, the boundary element method (BEM) has been employed by several papers, for instance, for solving magneto-thermoviscoelastic problems [20], micropolar piezothermoelastic problems [21], bio-heat transfer problems [22], micropolar FGA composite problems [23], porothermoelastic wave propagation problems [24], size-dependent thermopiezoelectric problems [25], and photothermal stress wave propagation problems [26]. One of the most commonly used methods for converting a domain integral to a boundary integral is the so-called dual reciprocity BEM (DRBEM). This method was developed by Nardini and Brebbia [27] for two-dimensional (2D) elastodynamics, but it has since been extended to a wide range of problems in which the domain integral can account for linear–nonlinear static–dynamic phenomena. More historical context and applications of the dual reciprocity boundary element approach [28] to nonlinear diffusion problems [29], general field equations [30], and spontaneous ignition problems [31].

The main goal of this article is to propose a DRBEM for solving problems of rotating FGA fiber-reinforced magneto-thermoelastic composites. The DRBEM was used with an implicit–implicit algorithm to obtain the solution for the considered governing equations. The numerical results show how functionally graded parameters and rotation affect magnetic thermal stresses in the fiber direction. The numerical results confirm the validity and accuracy of our proposed model.

2 Formulation of the problem

Figure 1 depicts a Cartesian coordinate system $Ox_1x_2x_3$. In the presence of a spatially varying heat source, we will consider an FGA fiber-reinforced thermoelastic composite in the presence of a primary magnetic field H_0 acting in the fiber-direction x_1-axis and rotating about it with a constant angular velocity. The anisotropic properties of the structure material have a gradient in the fiber direction. Because we are only concerned with the generalized 2D deformation problem in the x_2x_3-plane only, all variables are constant along the x_1-axis.

The governing equations of generalized magneto-thermoelastic problems in a rotating FGA fiber-reinforced structures can be written as [32]:

$$\sigma_{ab,b} + \tau_{ab,b} - \rho'\omega^2 x_a = \rho'\ddot{u}_a\ , \tag{1}$$

$$\sigma_{ab} = [C'_{abfg}u_{f,g} - \beta'_{ab}(T - T_0 + \tau_1\dot{T})], \tag{2}$$

$$\begin{aligned}\tau_{ab} &= \mu'(\tilde{h}_a H_b + \tilde{h}_b H_a - \delta_{ba}(\tilde{h}_f H_f)),\\ \tilde{h}_a &= (\nabla\times(u\times H))_a,\end{aligned} \tag{3}$$

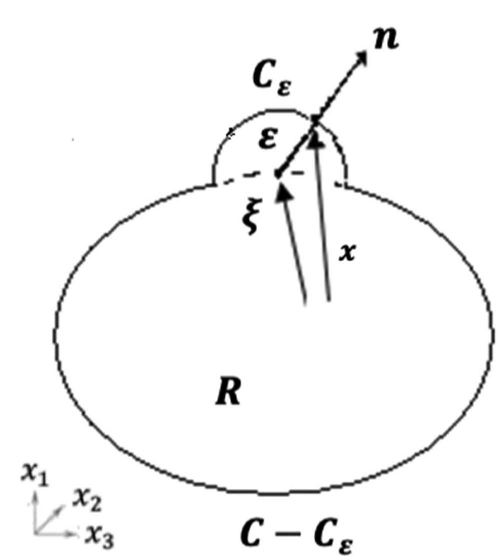

Figure 1: Geometry of the considered problem.

$$[\delta_{1j}k'_{ab} + \delta_{2j}k'^{\star}_{ab}]T_{,ab} = -\delta_{2j}k'_{ab}\dot{T}_{,ab} + \beta'_{ab}T_0[\text{Å}\delta_{1j}\dot{u}_{a,b} + (\tau_0 + \delta_{2j})\ddot{u}_{a,b}] + \rho' c[\delta_{1j}\dot{T} + (\tau_0 + \delta_{1j}\tau_2 + \delta_{2j})\ddot{T}]. \quad (4)$$

As shown in Figure 1, the boundary C is deformed by a small circular region with radius ε surrounding the load point ξ. Therefore, according to Fahmy [33], the initial and boundary conditions are supposed to be expressed as

$$u_f(x_2, x_3, 0) = \dot{u}_f(x_2, x_3, 0) = 0 \text{ for } (x_2, x_3) \in R \cup C, \quad (5)$$

$$u_f(x_2, x_3, \tau) = \Psi_f(x_2, x_3, \tau) \text{ for } (x_2, x_3) \in \boldsymbol{C_\varepsilon}, \quad (6)$$

$$\bar{t}_a(x_2, x_3, \tau) = \delta_f(x_2, x_3, \tau) \text{ for } (x_2, x_3) \in \boldsymbol{C} - \boldsymbol{C_\varepsilon},\ \tau > 0, \quad C = \boldsymbol{C_\varepsilon} \cup \boldsymbol{C} - \boldsymbol{C_\varepsilon}, \boldsymbol{C_\varepsilon} \cap \boldsymbol{C} - \boldsymbol{C_\varepsilon} = \varnothing, \quad (7)$$

$$T(x_2, x_3, \tau) = \dot{T}(x_2, x_3, \tau) = 0 \text{ for } (x_2, x_3) \in R \cup C, \quad (8)$$

$$T(x_2, x_3, \tau) = f(x_2, x_3, \tau) \text{ for } (x_2, x_3) \in \boldsymbol{C_\varepsilon},\ \tau > 0, \quad (9)$$

$$q(x_2, x_3, \tau) = \bar{h}(x_2, x_3, \tau)\ for\ (x_2, x_3) \in \boldsymbol{C} - \boldsymbol{C_\varepsilon},\ \tau > 0, \quad C = \boldsymbol{C_\varepsilon} \cup \boldsymbol{C} - \boldsymbol{C_\varepsilon}, \boldsymbol{C_\varepsilon} \cap \boldsymbol{C} - \boldsymbol{C_\varepsilon} = \varnothing. \quad (10)$$

For functionally graded materials, the parameters $C'_{abfg}(C'_{abfg} = C'_{fgab} = C'_{bafg})$, $\beta'_{ab}(\beta'_{ab} = \beta'_{ba})$, μ', ρ', and $k'_{ab}(k'_{23})^2 - k'_{22}k'_{33} < 0)$ are space dependent. We focused our attention in this article on the effect of inhomogeneity along the $0x$ direction. As a result, we replace these quantities by $C_{abfg}f(x)$, $\beta_{ab}f(x)$, $\mu f(x)$, $\rho f(x)$, and $k_{ab}f(x)$, where C_{abfg}, β_{ab}, μ, ρ, and k_{ab} are assumed to be constants and $f(x)$ is a given nondimensional function of space variable x. We use the formula $f(x) = (x + 1)^m$, where m is a dimensionless constant.

Thus, the governing equations (1)–(4) can be written as

$$\sigma_{ab,b} + \tau_{ab,b} - \rho(x + 1)^m\omega^2 x_a = \rho(x + 1)^m\ddot{u}_a, \quad (11)$$

$$\sigma_{ab} = (x + 1)^m[C_{abfg}u_{f,g} - \beta_{ab}(T - T_0 + \tau_1\dot{T})], \quad (12)$$

$$\tau_{ab} = \mu(x + 1)^m(\tilde{h}_a H_b + \tilde{h}_b H_a - \delta_{ba}(\tilde{h}_f H_f)), \quad (13)$$

$$[\delta_{1j}k_{ab} + \delta_{2j}k^{\star}_{ab}]T_{,ab} = -\delta_{2j}k_{ab}\dot{T}_{,ab} + \beta_{ab}T_0[\text{Å}\delta_{1j}\dot{u}_{a,b} + (\tau_0 + \delta_{2j})\ddot{u}_{a,b}] + \rho c[\delta_{1j}\dot{T} + (\tau_0 + \delta_{1j}\tau_2 + \delta_{2j})\ddot{T}]. \quad (14)$$

To study the pure anisotropic fiber-reinforced effect, we considered that

$$C_{abfg}u_{f,g} = [\bar{\lambda}e_{kk}\delta_{ab} + 2\mu_T e_{ab} + \alpha(a_k a_m e_{km}\delta_{ab} + a_a a_b e_{kk}) + 2(\mu_L - \mu_T)(a_a a_k e_{kb} + a_b a_k e_{ka}) + \beta a_k a_m e_{km} a_a a_b],$$

where the reinforcement parameters α, β, and $(\mu_L - \mu_T)$ introduce strongly anisotropic *behavior* in the considered structure, and isotropic behavior can be achieved considering the following condition $\alpha = \beta = (\mu_L - \mu_T) = 0$.

3 Numerical implementation

We can write equation (11) using equations (12) and (13) as follows

$$L_{gb}u_f = \rho\ddot{u}_a - (D_a T - \rho\omega^2 x_a) = f_{gb}, \quad (15)$$

where

$$L_{gb} = D_{abf}\frac{\partial}{\partial x_b} + D_{af} + \Lambda D_{a1f}, D_{abf} = C_{abfg}\aleph\varepsilon,\ \varepsilon = \frac{\partial}{\partial x_g},$$

$$D_{af} = \mu H_0^2\left(\frac{\partial}{\partial x_a} + \delta_{a1}\Lambda\right)\frac{\partial}{\partial x_f},$$

$$D_a = -\beta_{ab}\left(\frac{\partial}{\partial x_b} + \delta_{b1}\Lambda + \tau_1\left(\frac{\partial}{\partial x_b} + \Lambda\right)\frac{\partial}{\partial \tau}\right),\ \Lambda = \frac{m}{x + 1},$$

$$f_{gb} = \rho\ddot{u}_a - (D_a T - \rho\omega^2 x_a).$$

The field equations can now be expressed as

$$L_{gb}u_f = f_{gb}, \quad (16)$$

$$L_{ab}T = f_{ab}, \quad (17)$$

where the operators L_{gb} and f_{gb} have already been defined and the operators L_{ab} and f_{ab} have been defined as:

$$L_{ab} = [\delta_{1j}k_{ab} + \delta_{2j}k^{\star}_{ab}]\frac{\partial}{\partial x_a}\frac{\partial}{\partial x_b}, \quad (18)$$

$$f_{ab} = -\delta_{2j}k_{ab}\dot{T}_{,ab} + \rho c(x + 1)^m[\delta_{1j}\dot{T} + (\tau_0 + \delta_{1j}\tau_2 + \delta_{2j})\ddot{T}] + T_0\beta_{ab}(\text{Å}\delta_{1j}\dot{u}_{a,b} + (\tau_0 + \delta_{2j})\ddot{u}_{a,b}). \quad (19)$$

By applying the weighted residual technique to equation (16), we obtain

$$\int_R (L_{gb}u_f - f_{gb})u^{\star}_{da}\mathrm{d}R = 0. \quad (20)$$

The fundamental solution $u^{\star}_{df}$ is now taken as the weighting function as

$$L_{gb}u^{\star}_{df} = -\delta_{ad}\delta(x, \xi). \quad (21)$$

Also, the fundamental solution of traction can be expressed as

$$t^{\star}_{da} = C_{abfg}\aleph u^{\star}_{df,g}n_b, \quad (22)$$

where the traction can be expressed as

$$t_a = \frac{\bar{t}_a}{(x + 1)^m} = (C_{abfg}\aleph u_{f,g} - \beta_{ab}(T + \tau_1\dot{T}))n_b. \quad (23)$$

Using Dirac's sifting property and integration by parts on equation (20), we obtain

$$u_d(\xi) = \int_C (u^{\star}_{da} t_a - t^{\star}_{da} u_a + u^{\star}_{da} \beta_{ab} T n_b) \mathrm{d}C - \int_R f_{gb} u^{\star}_{da} \mathrm{d}R. \tag{24}$$

The fundamental solution $T^{\star}$ of the heat operator L_{ab} can be expressed as

$$L_{ab} T^{\star} = -\delta(x, \xi). \tag{25}$$

By using the weighted residual technique and applying integration by parts to equation (17), we obtain

$$\int_R (L_{ab} T T^{\star} - L_{ab} T^{\star} T) \mathrm{d}R = \int_C (q^{\star} T - q T^{\star}) \mathrm{d}C\ , \tag{26}$$

in which the heat fluxes are

$$q = -k_{ab} T_{,b} n_a, \tag{27}$$

$$q^{\star} = -k_{ab} T^{\star}_{,b} n_a. \tag{28}$$

Using Dirac's sifting property and integration by parts on equation (26), we obtain

$$T(\xi) = \int_C (q^{\star} T - q T^{\star}) dC - \int_R f_{ab} T^{\star} dR. \tag{29}$$

The coupled thermoelastic integral formulae of equations (24) and (29) are

$$\begin{bmatrix} u_d(\xi) \\ T(\xi) \end{bmatrix} = \int_C \left\{ -\begin{bmatrix} t^{\star}_{da} & -u^{\star}_{da} \beta_{ab} n_b \\ 0 & -q^{\star} \end{bmatrix} \begin{bmatrix} u_a \\ T \end{bmatrix} + \begin{bmatrix} u^{\star}_{da} & 0 \\ 0 & -T^{\star} \end{bmatrix} \begin{bmatrix} t_a \\ q \end{bmatrix} \right\} \mathrm{d}C - \int_R \begin{bmatrix} u^{\star}_{da} & 0 \\ 0 & -T^{\star} \end{bmatrix} \begin{bmatrix} f_{gb} \\ -f_{ab} \end{bmatrix} \mathrm{d}R. \tag{30}$$

In contract notation, we can write the following elastic and thermal variables:

$$U_A = \begin{cases} u_a & a = A = 1,\ 2,\ 3 \\ T & A = 4 \end{cases} \tag{31}$$

$$\mathrm{T}_A = \begin{cases} t_a & a = A = 1,\ 2,\ 3 \\ q & A = 4 \end{cases} \tag{32}$$

$$U^{\star}_{DA} = \begin{cases} u^{\star}_{da} & d = D = 1,\ 2,\ 3;\ a = A = 1,\ 2,\ 3 \\ 0 & d = D = 1,\ 2,\ 3;\ A = 4 \\ 0 & D = 4;\ a = A = 1,\ 2,\ 3 \\ -T^{\star} & D = 4;\ A = 4 \end{cases} \tag{33}$$

$$\tilde{T}^{\star}_{DA} = \begin{cases} t^{\star}_{da} & d = D = 1,\ 2,\ 3;\ a = A = 1,\ 2,\ 3 \\ -\tilde{u}^{\star}_d & d = D = 1,\ 2,\ 3;\ A = 4 \\ 0 & D = 4;\ a = A = 1,\ 2,\ 3 \\ -q^{\star} & D = 4;\ A = 4 \end{cases} \tag{34}$$

$$\tilde{u}^{\star}_d = u^{\star}_{da} \beta_{af} n_f. \tag{35}$$

The thermoelastic representation formula (30) in terms of contracted notation can be expressed as:

$$U_D(\xi) = \int_C (U^{\star}_{DA} \mathrm{T}_A - \tilde{T}_{DA} U_A) \mathrm{d}C - \int_R U^{\star}_{DA} S_A \mathrm{d}R, \tag{36}$$

where

$$S_A = S^0_A + S^T_A + S^{\dot{T}}_A + S^{\ddot{T}}_A + S^{\dot{u}}_A + S^{\ddot{u}}_A \tag{37}$$

in which

$$S^0_A = \begin{cases} \rho \omega^2 x_a & A = 1,\ 2,\ 3 \\ 0 & A = 4, \end{cases} \tag{38}$$

$$S^T_A = \omega_{AF} U_F \text{ with } \omega_{AF} = \begin{cases} -D_a\ A = 1,\ 2,\ 3; & F = 4 \\ 0 & \text{otherwise,} \end{cases} \tag{39}$$

$$S^{\dot{T}}_A = \left(\delta_{2j} k_{ab} \frac{\partial}{\partial x_a} \frac{\partial}{\partial x_b} - \rho c (x + 1)^m \delta_{1j} \right) \delta_{AF} \dot{U}_F \text{ with } \delta_{AF} = \begin{cases} 1 & A = 4; F = 4 \\ 0 & \text{otherwise,} \end{cases} \tag{40}$$

$$S^{\ddot{T}}_A = -\rho c (x + 1)^m (\tau_0 + \delta_{1j} \tau_2 + \delta_{2j}) \delta_{AF} \ddot{U}_F, \tag{41}$$

$$S^{\dot{u}}_A = -T_0 \mathring{A} \delta_{1j} \beta_{fg} \varepsilon \dot{U}_F, \tag{42}$$

$$S^{\ddot{u}}_A = \Finv \ddot{U}_F \quad \text{with } \Finv = \begin{cases} \rho & A = 1,\ 2,\ 3;\ F = 1,\ 2,\ 3, \\ -T_0 \beta_{fg} (\tau_0 + \delta_{2j}) \varepsilon & A = 4;\ f = F = 4 \end{cases} \tag{43}$$

In matrix form, the coupled thermoelastic integral formulae (30) can be written as

$$[S_A] = \begin{bmatrix} \rho \omega^2 x_a \\ 0 \end{bmatrix} + \begin{bmatrix} -D_a T \\ 0 \end{bmatrix} + \left(\delta_{2j} k_{ab} \frac{\partial}{\partial x_a} \frac{\partial}{\partial x_b} - \rho c (x + 1)^m \delta_{1j} \right) \begin{bmatrix} 0 \\ \dot{T} \end{bmatrix} - \rho c (x + 1)^m (\tau_0 + \delta_{1j} \tau_2 + \delta_{2j}) \begin{bmatrix} 0 \\ \ddot{T} \end{bmatrix} - T_0 \delta_{1j} \begin{bmatrix} 0 \\ \beta_{fg} \dot{u}_{f,g} \end{bmatrix} + \begin{bmatrix} \rho \ddot{u}_a \\ -T_0 \beta_{fg} (\tau_0 + \delta_{2j}) \ddot{u}_{f,g} \end{bmatrix}, \tag{44}$$

where

$$S_A \approx \sum_{q=1}^{N} f_{AN}^{q} \alpha_N^{q}. \tag{45}$$

Now, equation (36) may be expressed as

$$U_D(\xi) = \int_C (U_{DA}^{\star} T_A - \tilde{T}_{DA}^{\star} U_A) \mathrm{d}C - \sum_{q=1}^{N} \int_R U_{DA}^{\star} f_{AN}^{q} \mathrm{d}R \alpha_N^{q}. \tag{46}$$

Now, we may solve the following equations:

$$L_{gb} u_{fn}^{q} = f_{an}^{q}, \tag{47}$$

$$L_{ab} T^{q} = f_{pj}^{q}. \tag{48}$$

According to Fahmy [34], we can write

$$u_{dn}^{q}(\xi) = \int_C (u_{da}^{\star} t_{an}^{q} - t_{da}^{\star} u_{an}^{q}) \mathrm{d}C - \int_R u_{da}^{\star} f_{an}^{q} \mathrm{d}R, \tag{49}$$

$$T^{q}(\xi) = \int_C (q^{\star} T^{q} - q^{q} T^{\star}) \mathrm{d}C - \int_R f^{q} T^{\star} \mathrm{d}R. \tag{50}$$

The coupled thermoelastic representation formulae can be written as

$$U_{DN}^{q}(\xi) = \int_C (U_{DA}^{\star} T_{AN}^{q} - T_{DA}^{\star} U_{AN}^{q}) \mathrm{d}C - \int_R U_{DA}^{\star} f_{AN}^{q} \mathrm{d}R. \tag{51}$$

By using equation (51), we can write the representation formula (46) as

$$U_D(\xi) = \int_C (U_{DA}^{\star} T_A - \check{T}_{DA}^{\star} U_A) \mathrm{d}C + \sum_{q=1}^{N} \left(U_{DN}^{q}(\xi) + \int_C (T_{DA}^{\star} U_{AN}^{q} - U_{DA}^{\star} T_{AN}^{q}) \mathrm{d}C \right) \alpha_N^{q}. \tag{52}$$

Now, to calculate interior stresses, we differentiate equation (52) with respect to ξ_l as follows:

$$\frac{\partial U_D(\xi)}{\partial \xi_l} = -\int_C (U_{DA,l}^{\star} T_A - \check{T}_{DA,l}^{\star} U_A) \mathrm{d}C + \sum_{q=1}^{N} \left(\frac{\partial U_{DN}^{q}(\xi)}{\partial \xi_l} - \int_C (T_{DA,l}^{\star} U_{AN}^{q} - U_{DA,l}^{\star} T_{AN}^{q}) \mathrm{d}C \right) \alpha_N^{q}. \tag{53}$$

Now, the representation formula (52) may be expressed as [34]

$$\check{\zeta} U - \eta T = (\zeta \check{U} - \eta \check{\wp}) \alpha. \tag{54}$$

According to Gaul et al. [35], we can write

$$U_F \approx \sum_{q=1}^{N} f_{FD}^{q}(x) \gamma_D^{q}, \tag{55}$$

$$\dot{U}_F \approx \sum_{q=1}^{N} f_{FD}^{q}(x) \tilde{\gamma}_D^{q}, \tag{56}$$

where f_{FD}^{q} are tensor functions and γ_D^{q} and $\tilde{\gamma}_D^{q}$ are unknown coefficients.

Also, the corresponding gradients are approximated as

$$U_{F,g} \approx \sum_{q=1}^{N} f_{FD,g}^{q}(x) \gamma_K^{q}, \tag{57}$$

$$\dot{U}_{F,g} \approx \sum_{q=1}^{N} f_{FD,g}^{q}(x) \tilde{\gamma}_D^{q}, \tag{58}$$

where

$$S_A^{T} = \sum_{q=1}^{N} S_{AD}^{T,q} \gamma_D^{q}, \tag{59}$$

$$S_A^{\dot{u}} = -T_0 \mathring{A} \delta_{1j} \beta_{fg} \varepsilon \sum_{q=1}^{N} S_{AD}^{\dot{u},q} \tilde{\gamma}_D^{q}, \tag{60}$$

in which

$$S_{AD}^{T,q} = S_{AF} f_{FD,g}^{q}, \tag{61}$$

$$S_{AD}^{\dot{u},q} = S_{FA} f_{FD,g}^{q}. \tag{62}$$

According to the point collocation technique of Gaul et al. [35], we can write equations (45), (55), and (56) as

$$\check{S} = J\alpha, \; U = J'\gamma, \; \dot{U} = J'\tilde{\gamma}. \tag{63}$$

Also, equations (40), (41), (43), (59), and (60) can be written as [35]

$$\check{S}^{\dot{T}} = \left(\delta_{2j} k_{ab} \frac{\partial}{\partial x_a} \frac{\partial}{\partial x_b} - \rho c (x+1)^m \delta_{1j} \right) \delta_{AF} \dot{U}, \tag{64}$$

$$\check{S}^{\ddot{T}} = -c\rho (x+1)^m (\tau_0 + \delta_{1j}\tau_2 + \delta_{2j}) \delta_{AF} \ddot{U}, \tag{65}$$

$$\check{S}^{\ddot{u}} = \tilde{A} \ddot{U}, \tag{66}$$

$$\check{S}^{T} = \mathcal{B}^{T} \gamma, \tag{67}$$

$$\check{S}^{\dot{u}} = -T_0 \mathring{A} \delta_{1j} \beta_{fg} \varepsilon \mathcal{B}^{\dot{u}} \tilde{\gamma}. \tag{68}$$

The solution of the system (63) for α, γ, and $\tilde{\gamma}$ yields

$$\alpha = J^{-1} \check{S} \; \gamma = J'^{-1} U \; \tilde{\gamma} = J'^{-1} \dot{U}, \tag{69}$$

where

$$\alpha = J^{-1} \Bigg(\check{S}^{0} + \mathcal{B}^{T} J'^{-1} U + \Bigg[\left(\delta_{2j} k_{ab} \frac{\partial}{\partial x_a} \frac{\partial}{\partial x_b} - \rho c (x+1)^m \delta_{1j} \right) \delta_{AF} - T_0 \mathring{A} \delta_{1j} \beta_{fg} \varepsilon \mathcal{B}^{\dot{u}} J'^{-1} \Bigg] \dot{U}. + [\tilde{A} - c\rho (x+1)^m (\tau_0 + \delta_{1j}\tau_2 + \delta_{2j}) \delta_{AF}] \ddot{U} \Bigg). \tag{70}$$

Substituting equation (70) into equation (54), we obtain [36]:

$$\widetilde{M}\ddot{U} + \widetilde{\Gamma}\dot{U} + \widetilde{K}U = \widetilde{\mathbb{Q}}\,, \tag{71}$$

$$\widetilde{X}\ddot{T} + \widetilde{A}\dot{T} + \widetilde{B}T = \widetilde{\mathbb{Z}}\ddot{U} + \widetilde{\mathbb{R}}\dot{U}, \tag{72}$$

where $V = (\eta\check{\wp} - \zeta\check{U})J^{-1}$, $\widetilde{M} = V\tilde{A}$, $\widetilde{X} = -\rho c(x+1)^m(\tau_0 + \delta_{1j}\tau_2 + \delta_{2j})$,

$\widetilde{K} = \tilde{\zeta} + V\mathcal{B}^T J'^{-1}$, $\mathbb{Q} = \eta T + V\check{S}^0$, $\widetilde{B} = \delta_{1j}k_{ab} + \delta_{2j}k^{\star}_{ab}$,

$\widetilde{\Gamma} = V\left[\left(k_{ab}\frac{\partial}{\partial x_a}\frac{\partial}{\partial x_b} - c\rho\delta_{1j}\right)\delta_{AF} - T_0\mathring{A}_{1j}\beta_{fg}\varepsilon\mathcal{B}^{\dot{u}}J'^{-1}\right]$, $\widetilde{\mathbb{R}} = T_0\beta_{ab}\mathring{A}\delta_{1j}$,

$\widetilde{\mathbb{Z}} = T_0\beta_{ab}(\tau_0 + \delta_{2j})$, $\widetilde{A} = \left(\delta_{2j}k_{ab}\frac{\partial}{\partial x_a}\frac{\partial}{\partial x_b} - \rho c(x+1)^m\delta_{1j}\right)\delta_{AF}$,

where the vectors $\ddot{U}$, $\dot{U}$, U, T, and $\widetilde{\mathbb{Q}}$ are acceleration, velocity, displacement, temperature, and external force, respectively, the matrices V, $\widetilde{M}$, $\widetilde{\Gamma}$, $\widetilde{A}$, $\widetilde{B}$, and $\widetilde{K}$ are volume, mass, damping, capacity, conductivity, and stiffness, respectively, $\widetilde{\mathbb{Z}}$ and $\widetilde{\mathbb{R}}$ are coupling matrices, and $\widetilde{X}$ is a vector suggested by Green and Lindsay [5].

Thus, the governing equations can be expressed as [36]:

$$\widetilde{M}\ddot{U}_{n+1} + \widetilde{\Gamma}\dot{U}_{n+1} + \widetilde{K}U_{n+1} = \widetilde{\mathbb{Q}}^{p}_{n+1}, \tag{73}$$

$$\widetilde{X}\ddot{T}_{n+1} + \widetilde{A}\dot{T}_{n+1} + \widetilde{B}T_{n+1} = \widetilde{\mathbb{Z}}\ddot{U}_{n+1} + \widetilde{\mathbb{R}}\dot{U}_{n+1}, \tag{74}$$

where $\widetilde{\mathbb{Q}}^{p}_{n+1} = \eta T^{p}_{n+1} + V\check{S}^0$ and T^{p}_{n+1} is the predicted temperature.

By applying the trapezoidal rule and integrating equation (71), we obtain

$$\begin{aligned}\dot{U}_{n+1} &= \dot{U}_n + \frac{\Delta\tau}{2}(\ddot{U}_{n+1} + \ddot{U}_n)\\ &= \dot{U}_n + \frac{\Delta\tau}{2}[\ddot{U}_n + \widetilde{M}^{-1}(\widetilde{\mathbb{Q}}^{p}_{n+1} - \widetilde{\Gamma}\dot{U}_{n+1} - \widetilde{K}U_{n+1})],\end{aligned} \tag{75}$$

$$\begin{aligned}U_{n+1} &= U_n + \frac{\Delta\tau}{2}(\dot{U}_{n+1} + \dot{U}_n)\\ &= U_n + \Delta\tau\dot{U}_n + \frac{\Delta\tau^2}{4}[\ddot{U}_n + \widetilde{M}^{-1}(\widetilde{\mathbb{Q}}^{p}_{n+1} - \widetilde{\Gamma}\dot{U}_{n+1} - \widetilde{K}U_{n+1})].\end{aligned} \tag{76}$$

From equation (75) we have

$$\dot{U}_{n+1} = \overline{\Upsilon}^{-1}\left[\dot{U}_n + \frac{\Delta\tau}{2}[\ddot{U}_n + \widetilde{M}^{-1}(\widetilde{\mathbb{Q}}^{p}_{n+1} - \widetilde{K}U_{n+1})]\right], \tag{77}$$

where $\overline{\Upsilon} = \left(I + \frac{\Delta\tau}{2}\widetilde{M}^{-1}\widetilde{\Gamma}\right)$.

Substituting equation (77) into equation (76), we have

$$\begin{aligned}U_{n+1} = U_n + \Delta\tau\dot{U}_n + \frac{\Delta\tau^2}{4}\Bigg[\ddot{U}_n + \widetilde{M}^{-1}\Bigg(\widetilde{\mathbb{Q}}^{p}_{n+1} - \widetilde{\Gamma}\bar{\Upsilon}^{-1}\Bigg[\dot{U}_n\\ + \frac{\Delta\tau}{2}[\ddot{U}_n + \widetilde{M}^{-1}(\widetilde{\mathbb{Q}}^{p}_{n+1} - \widetilde{K}U_{n+1})]\Bigg] - \widetilde{K}U_{n+1}\Bigg)\Bigg].\end{aligned} \tag{78}$$

Substituting $\dot{U}_{n+1}$ from equation (77) into equation (73) yields

$$\begin{aligned}\ddot{U}_{n+1} = \widetilde{M}^{-1}\Bigg[\widetilde{\mathbb{Q}}^{p}_{n+1} - \widetilde{\Gamma}\Bigg[\overline{\Upsilon}^{-1}\Bigg[\dot{U}_n + \frac{\Delta\tau}{2}[\ddot{U}_n + \widetilde{M}^{-1}(\widetilde{\mathbb{Q}}^{p}_{n+1}\\ - \widetilde{K}U_{n+1})]\Bigg]\Bigg] - \widetilde{K}U_{n+1}\Bigg].\end{aligned} \tag{79}$$

Through the integration of equation (72) with the trapezoidal rule, we obtain

$$\begin{aligned}\dot{T}_{n+1} &= \dot{T}_n + \frac{\Delta\tau}{2}(\ddot{T}_{n+1} + \ddot{T}_n)\\ &= \dot{T}_n + \frac{\Delta\tau}{2}(\widetilde{X}^{-1}[\widetilde{\mathbb{Z}}\ddot{U}_{n+1} + \widetilde{\mathbb{R}}\dot{U}_{n+1} - \widetilde{A}\dot{T}_{n+1} - \widetilde{B}T_{n+1}] + \ddot{T}_n),\end{aligned} \tag{80}$$

$$\begin{aligned}T_{n+1} &= T_n + \frac{\Delta\tau}{2}(\dot{T}_{n+1} + \dot{T}_n)\\ &= T_n + \Delta\tau\dot{T}_n + \frac{\Delta\tau^2}{4}(\ddot{T}_n + \widetilde{\mathrm{X}}^{-1}[\widetilde{\mathbb{Z}}\ddot{U}_{n+1} + \widetilde{\mathbb{R}}\dot{U}_{n+1} - \widetilde{A}\dot{T}_{n+1} - \widetilde{B}T_{n+1}]).\end{aligned} \tag{81}$$

Now, we can write equation (80) as

$$\dot{T}_{n+1} = \Upsilon^{-1}\left[\dot{T}_n + \frac{\Delta\tau}{2}(\widetilde{\mathrm{X}}^{-1}[\widetilde{\mathbb{Z}}\ddot{U}_{n+1} + \widetilde{\mathbb{R}}\dot{U}_{n+1} - \widetilde{\mathrm{B}}T_{n+1}] + \ddot{T}_n)\right], \tag{82}$$

where $\Upsilon = \left(I + \frac{1}{2}\widetilde{\mathrm{A}}\Delta\tau\widetilde{\mathrm{X}}^{-1}\right)$

Substituting equation (82) into equation (81), we obtain

$$\begin{aligned}T_{n+1} = T_n + \Delta\tau\dot{T}_n + \frac{\Delta\tau^2}{4}(\ddot{T}_n + \widetilde{\mathrm{X}}^{-1}[\widetilde{\mathbb{Z}}\ddot{U}_{n+1} + \widetilde{\mathbb{R}}\dot{U}_{n+1}\\ - \widetilde{\mathrm{A}}\left(\Upsilon^{-1}\left[\dot{T}_n + \frac{\Delta\tau}{2}(\widetilde{\mathrm{X}}^{-1}[\widetilde{\mathbb{Z}}\ddot{U}_{n+1} + \widetilde{\mathbb{R}}\dot{U}_{n+1} - \widetilde{B}T_{n+1}] + \ddot{T}_n)\right]\right) - \widetilde{B}T_{n+1}]).\end{aligned} \tag{83}$$

Substituting equation (82) into equation (74) we obtain

$$\begin{aligned}\ddot{T}_{n+1} = \widetilde{\mathrm{X}}^{-1}\Bigg[\widetilde{\mathbb{Z}}\ddot{U}_{n+1} + \widetilde{\mathbb{R}}\dot{U}_{n+1}\\ - \widetilde{\mathrm{A}}\left(\Upsilon^{-1}\left[\dot{T}_n + \frac{\Delta\tau}{2}(\widetilde{\mathrm{X}}^{-1}[\widetilde{\mathbb{Z}}\ddot{U}_{n+1} + \widetilde{\mathbb{R}}\dot{U}_{n+1} - \widetilde{B}T_{n+1}] + \ddot{T})\right]\right) - \widetilde{B}T_{n+1}\Bigg].\end{aligned} \tag{84}$$

We use the predictor-corrector approach to solve equations (78) and (83), as follows:

Step 1. Predict the displacement field: $U^{p}_{n+1} = U_n$

Step 2. Substitute for $\dot{U}_{n+1}$ and $\ddot{U}_{n+1}$ from equations (75) and (73), respectively, in equation (83) and solve the temperature field equation that results.

Step 3. The predicted displacement and computed temperature are used to correct the displacement field.

Step 4. Equations (77), (79), (82), and (84) are used to calculate $\dot{U}_{n+1}$, $\ddot{U}_{n+1}$, $\dot{T}_{n+1}$, and $\ddot{T}_{n+1}$, respectively.

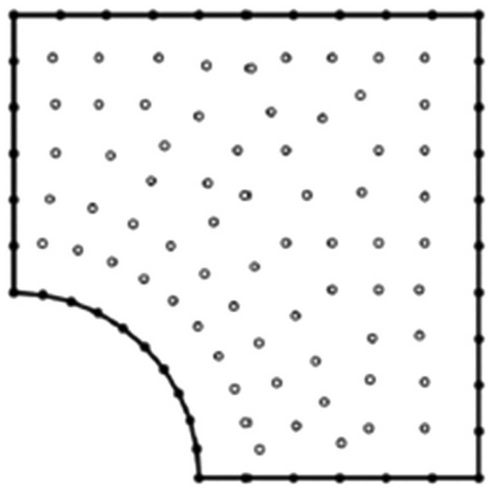

Figure 2: Boundary element model of the considered problem.

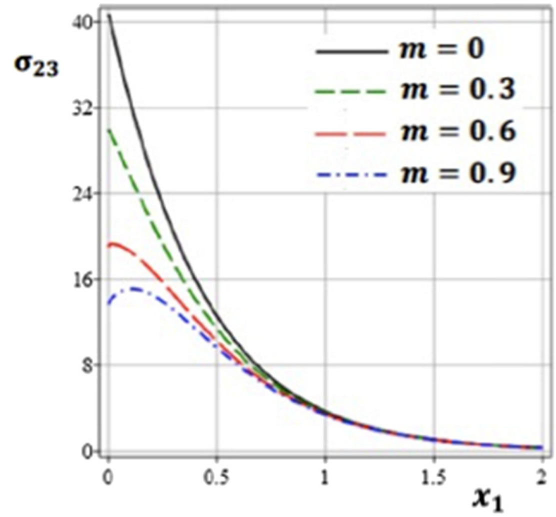

Figure 4: Variation of the thermal stress σ_{23} along x_1-axis for different values of the functionally graded parameter.

4 Numerical results and discussion

The findings of this work can be used in a wide range of rotating FGA fiber-reinforced magneto-thermoelastic composites. This work also improved the technique of Fahmy [33] by implementing the procedure of Farhat et al. [36] into the current study's DRBEM code.

In this article, we considered the following properties of pure copper: $\lambda_0 = 5.65 \times 10^{10}$ N m^{-2}, $\mu_T = 2.46 \times 10^{10}$ N m^{-2}, $\mu_L = 5.66 \times 10^{10}$ N m^{-2}, $\beta = 220.9 \times 10^{10}$ Nm^{-2}, $\rho = 2{,}660$ kg m^{-3}, $\tau_1 = 0.2$ s, and $\tau_2 = 0.2$ s, where the reinforcement parameters α, β, and $(\mu_L - \mu_T)$ introduce anisotropic behavior in the considered structure.

The domain boundary of the considered problem has been discretized into 42 boundary elements and 68 internal points, as illustrated in Figure 2.

Figures 3–5 display the thermal stresses σ_{22}, σ_{23}, and σ_{33} variations along x_1-axis for various functionally graded parameter values. These figures show that the functionally graded parameter has a significant effect on thermal stresses.

Figures 6–8 display the thermal stresses σ_{22}, σ_{23}, and σ_{33} variations along x_1-axis for various uniform angular velocity values. These figures demonstrate that rotation has a significant effect on thermal stresses.

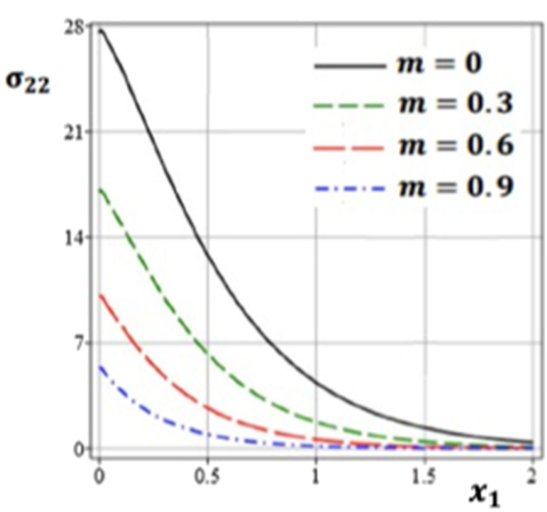

Figure 3: Variation of the thermal stress σ_{22} along x_1-axis for different values of the functionally graded parameter.

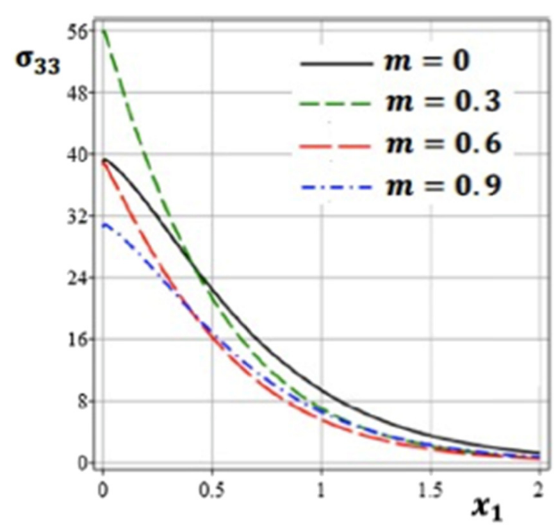

Figure 5: Variation of the thermal stress σ_{33} along x_1-axis for different values of the functionally graded parameter.

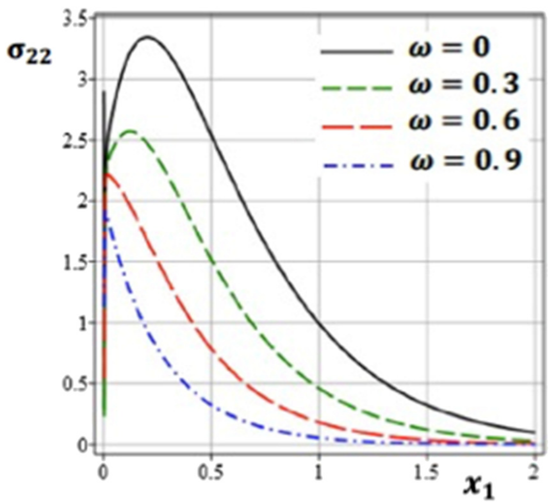

Figure 6: Variation of the thermal stress σ_{22} along x_1-axis for different values of rotation parameter.

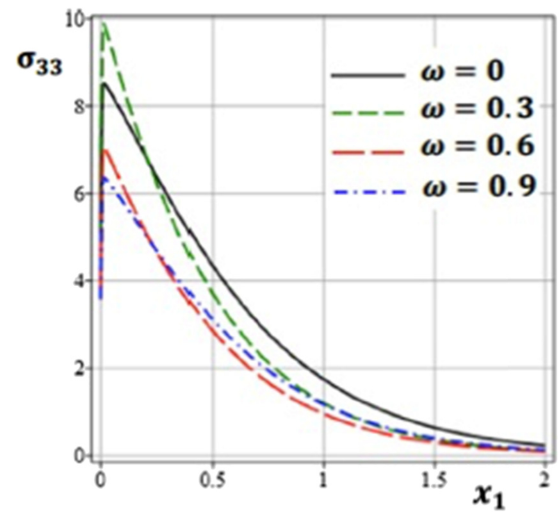

Figure 8: Variation of the thermal stress σ_{33} along x_1-axis for different values of rotation parameter.

Table 1 shows a comparison of required computer resources for the current dual reciprocity BEM results, FDM results of Pazera and Jędrysiak [37], and FEM results of Xiong and Tian [38] of modeling of rotating FGA fiber-reinforced magneto-thermoelastic composites.

For comparison, only one-dimensional results with ones previously known from the literature were chosen. Figure 9 depicts the evolution of the one-dimensional thermal stress σ_{22} with time for various techniques in the special example under consideration. We were able to demonstrate the validity, accuracy, and efficiency of the proposed technique by comparing our one-dimensional dual reciprocity BEM results to those obtained

Table 1: A comparison of the required computer resources for modeling of rotating functionally graded anisotropic fiber-reinforced magnetothermoelastic composites

	BEM	FDM	FEM
Number of nodes	68	54,000	50,000
Number of elements	42	24,000	20,000
CPU time	2	220	200
Memory	1	200	180
Disk space	0	260	240
Accuracy of results	1	2.2	2.0

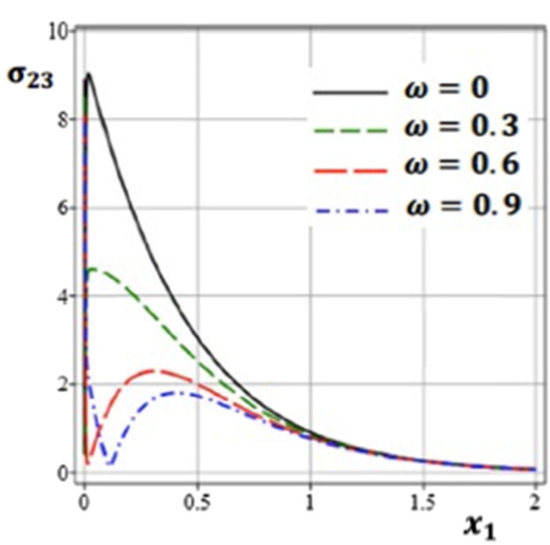

Figure 7: Variation of the thermal stress σ_{23} along x_1-axis for different values of rotation parameter.

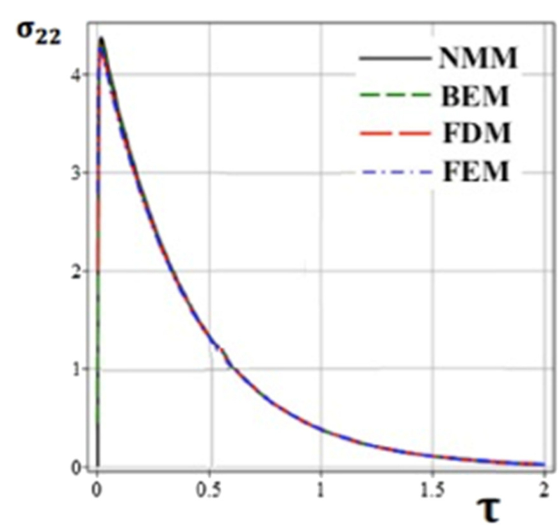

Figure 9: Variation of the thermal stress σ_{22} with time τ for different methods NMM, BEM, FDM, and FEM.

using the analytical normal mode method (NMM) [39], numerical finite difference method (FDM) [37], and numerical finite element method (FEM) [38]. According to these studies, the BEM results agree very well with the analytical NMM and numerical methods FDM and FEM used in the literature.

5 Conclusion

The primary goal of this article is to propose an implicit–implicit predictor–corrector DRBEM scheme for solving problems with rotating FGA fiber-reinforced magneto-thermoelastic composites. To steer the current research field toward the development of new functionally graded fiber-reinforced composites, we must successfully implement computerized numerical methods for solving and simulating complex nonlinear FGM problems. It is quite difficult to find analytical solutions to the governing equations. New numerical approaches to solving such equations must be developed to address this issue. To solve the theory's governing equations, we propose a new formulation of the DRBEM. Because of the benefits of the DRBEM approach, such as the ability to deal with issues involving complicated shapes that are difficult to deal with using standard methods, and the absence of the need for internal domain discretization. Low CPU utilization and memory storage are also required. As a result, the DRBEM is suitable for a wide range of advanced functionally graded fiber-reinforced composites. The numerical results are discussed in detail, with a focus on the effects of functionally graded parameters and rotation on the magneto-thermoelastic stresses of anisotropic fiber-reinforced composites in the fiber direction. To validate the proposed technique, the results were compared to those obtained using the analytical NMM, numerical FDM, and numerical FEM. According to the obtained results, the proposed DRBEM technique is more effective, precise, and stable than FDM or FEM. Computer scientists, material science researchers, engineers, and designers and developers of functionally graded fiber-reinforced composites may be interested in the current numerical results for our problem.

Acknowledgments: The authors would like to thank the Deanship of Scientific Research at Umm Al-Qura University for supporting this work by Grant Code: (22UQU4340548DSR02).

Funding information: This research was funded by [Deanship of Scientific Research at Umm Al-Qura University] grant number [22UQU4340548DSR02] And The APC was funded by [Deanship of Scientific Research at Umm Al-Qura University].

Conflict of interest: The authors declare no conflict of interest.

Data availability statement: All data generated or analyzed during this study are included in this published article

References

[1] Biot MA. Thermoelasticity and irreversible thermo-dynamics. J Appl Phys. 1956;27(3):240–53.
[2] Duhamel JMC. Some memoire sur les phenomenes thermo-mechanique. J de l'Ecole Polytech. 1837;15(25):1–57.
[3] Neumann F, Meyer OE. Vorlesungen Uber die theorie der elasticitat. Leipzig: B. G. Teubner; 1885.
[4] Lord HW, Shulman Y. A generalized dynamical theory of thermoelasticity. J Mech Phys Solids. 1967;15(5):299–309.
[5] Green AE, Lindsay KA. Thermoelasticity. J Elast. 1972;2:1–7.
[6] Green AE, Naghdi PM. On undamped heat waves in an elastic solid. J Therm Stresses. 1992;15(2):253–64.
[7] Green AE, Naghdi PM. Thermoelasticity without energy dissipation. J Elast. 1993;31(6):189–208.
[8] Armero F, Simo JC. A new unconditionally stable fractional step method for non-linear coupled thermomechanical problems. Int J Numer Methods Eng. 1992;35(4):737–66.
[9] Ezzat MA, Youssef HM. Generalized magneto-thermoelasticity in a perfectly conducting medium. Int J Solids Struct. 2005;42(24-25):6319–34.
[10] Abouelregal AE, Mohammed WW. Effects of nonlocal thermoelasticity on nanoscale beams based on couple stress theory. Math Methods Appl Sci. 2020. doi: 10.1002/mma.6764.
[11] Fahmy MA. A new boundary element formulation for modeling and simulation of three-temperature distributions in carbon nanotube fiber reinforced composites with inclusions. Math Methods Appl Sci. 2021. (Special issue title: Recent Advances in the Modelling of Nanotubes within Nano- Structures/Systems). doi: 10.1002/mma.7312.
[12] Fahmy MA. Boundary element algorithm for nonlinear modeling and simulation of three-temperature anisotropic generalized micropolar piezothermoelasticity with memory-dependent derivative. Int J Appl Mech. 2020;12(3):2050027. doi: 10.1142/S1758825120500271.
[13] Fahmy MA, Shaw S, Mondal S, Abouelregal AE, Lotfy K, Kudinov IA, et al. Boundary element modeling for simulation and optimization of three-temperature anisotropic micropolar magneto-thermoviscoelastic problems in porous smart structures using NURBS and genetic algorithm. Int J Thermophys. 2021;42(2):29.
[14] Fahmy MA. Boundary element modeling of 3T nonlinear transient magneto-thermoviscoelastic wave propagation problems in anisotropic circular cylindrical shells. Composite Struct. 2021;277:114655.

[15] Vel S, Batra RC. Three-dimensional analysis of transient thermal stresses in functionally graded plates. Int J Solids Struct. 2003;40(25):7181–96.
[16] Zhang XZ, Kitipornchа S, Liew KM, Lim CW, Peng LX. Thermal stresses around a circular hole in a functionally graded plate. J Therm Stresses. 2003;26(4):379–90.
[17] Ootao Y, Tanigawa Y. Transient thermoelastic analysis for a laminated composite strip with an interlayer of functionally graded material. J Therm Stresses. 2009;32(11):1181–97.
[18] Mirzaei D, Dehghan M. New implementation of MLBIE method for heat conduction analysis in functionally graded materials. Eng Anal Bound Elem. 2012;36(4):511–9.
[19] Rekik M, El-Borgi S, Ounaies Z. An embedded mixed-mode crack in a functionally graded magnetoelectroelastic infinite medium. Int J Solids Struct. 2012;49(5):835–45.
[20] Fahmy MA. A time-stepping DRBEM for magneto-thermo-viscoelastic interactions in a rotating nonhomogeneous anisotropic solid. Int J Appl Mech. 2011;3(4):1–24.
[21] Fahmy MA. A novel BEM for modeling and simulation of 3T nonlinear generalized anisotropic micropolar-thermoelasticity theory with memory dependent derivative. CMES-Computer Modeling Eng Sci. 2021;126(1):175–99.
[22] Fahmy MA. A new boundary element algorithm for a general solution of nonlinear space-time fractional dual-phase-lag bio-heat transfer problems during electromagnetic radiation. Case Stud Therm Eng. 2021;25:100918. doi: 10.1016/j.csite.2021.100918.
[23] Fahmy MA. A new boundary element algorithm for modeling and simulation of nonlinear thermal stresses in micropolar FGA composites with temperature-dependent properties. Adv Modeling Simul Eng Sci. 2021;8(6):1–23.
[24] Fahmy MA. A new bem for fractional nonlinear generalized porothermoelastic wave propagation problems. CMC-Computers Mater Continua. 2021;68(1):59–76.
[25] Fahmy MA. A new BEM modeling algorithm for size-dependent thermopiezoelectric problems in smart nanostructures CMC-computer. Mater Continua. 2021;69(1):931–44.
[26] Fahmy MA. Boundary element modeling of fractional nonlinear generalized photothermal stress wave propagation problems in FG anisotropic smart semiconductors. Eng Anal Bound Elem. 2022;134(1):665–79.
[27] Nardini D, Brebbia CA. A new approach to free vibration analysis using boundary elements. Appl Math Model. 1983;7(3):157–62.
[28] Partridge PW, Brebbia CA, Wrobel LC. The dual reciprocity boundary element method. Southampton: Computational Mechanics Publications; 1992.
[29] Wrobel LC, Brebbia CA. The dual reciprocity boundary element formulation for nonlinear diffusion problems. Computer Methods Appl Mech Eng. 1987;65(2):147–64.
[30] Partridge PW, Brebbia CA. Computer implementation of the BEM dual reciprocity method for the solution of general field equations. Commun Appl Num Methods. 1990;6(2):83–92.
[31] Partridge PW, Wrobel LC. The dual reciprocity boundary element method for spontaneous ignition. Int J Numer Methods Eng. 1990;30(5):953–63.
[32] Bagri A, Eslami MR. A unified generalized thermoelasticity; solution for cylinders and spheres. Int J Mech Sci. 2007;49(12):1325–35.
[33] Fahmy MA. A time-stepping DRBEM for the transient magneto-thermo-visco-elastic stresses in a rotating non-homogeneous anisotropic solid. Eng Anal Bound Elem. 2012;36(3):335–45.
[34] Fahmy MA. The effect of rotation and inhomogeneity on the transient magneto-thermo-visco-elastic stresses in an anisotropic solid. J Appl Mech. 2012;79(5):051015.
[35] Gaul L, Kögl M, Wagner M. Boundary element methods for engineers and scientists. Berlin: Springer-Verlag; 2003.
[36] Farhat C, Park KC, Dubois-Pelerin Y. An unconditionally stable staggered algorithm for transient finite element analysis of coupled thermoelastic problems. Computer Methods Appl Mech Eng. 1991;85(3Fe):349–65.
[37] Pazera E, Jędrysiak J. Effect of microstructure in thermoelasticity problems of functionally graded laminates. Composite Struct. 2018;202:296–303. doi: 10.1016/j.compstruct.2018.01.082.
[38] Xiong QL, Tian XG. Generalized magneto-thermo-microstretch response of a half-space with temperature-dependent properties during thermal shock. Lat Am J Solids Struct. 2015;12(13):2562–80.
[39] Deswal S, Punia BS, Kalkal KK. Thermodynamical interactions in a two-temperature dual-phase-lag micropolar thermoelasticity with gravity. Multidis Modeling Mater Struct. 2018;14(1):102–24.